Original article

MOLECULAR METABOLISM

RIPK1 is dispensable for cell death regulation in β-cells during hyperglycemia

Önay Veli[1,2,3], Öykü Kaya[1,2,3], Ana Beatriz Varanda[3,8], Ximena Hildebrandt[1,2,3], Peng Xiao[4], Yann Estornes[5,6], Matea Poggenberg[2], Yuan Wang[1,2,3], Manolis Pasparakis[3,7], Mathieu J.M. Bertrand[5,6], Henning Walczak[3,8], Alessandro Annibaldi[2], Alessandra K. Cardozo[4], Nieves Peltzer[1,2,3,*]

ABSTRACT

Objective: Receptor-interacting protein kinase 1 (RIPK1) orchestrates the decision between cell survival and cell death in response to tumor necrosis factor (TNF) and other cytokines. Whereas the scaffolding function of RIPK1 is crucial to prevent TNF-induced apoptosis and necroptosis, its kinase activity is required for necroptosis and partially for apoptosis. Although TNF is a proinflammatory cytokine associated with β-cell loss in diabetes, the mechanism by which TNF induces β-cell demise remains unclear.

Methods: Here, we dissected the contribution of RIPK1 scaffold versus kinase functions to β-cell death regulation using mice lacking RIPK1 specifically in β-cells (*Ripk1*$^{\beta\text{-}KO}$ mice) or expressing a kinase-dead version of RIPK1 (*Ripk1*^{D138N} mice), respectively. These mice were challenged with streptozotocin, a model of autoimmune diabetes. Moreover, *Ripk1*$^{\beta\text{-}KO}$ mice were further challenged with a high-fat diet to induce hyperglycemia. For mechanistic studies, pancreatic islets were subjected to various killing and sensitising agents.

Results: Inhibition of RIPK1 kinase activity (*Ripk1*^{D138N} mice) did not affect the onset and progression of hyperglycemia in a type 1 diabetes model. Moreover, the absence of RIPK1 expression in β-cells did not affect normoglycemia under basal conditions or hyperglycemia under diabetic challenges. *Ex vivo*, primary pancreatic islets are not sensitised to TNF-induced apoptosis and necroptosis in the absence of RIPK1. Intriguingly, we found that pancreatic islets display high levels of the antiapoptotic cellular FLICE-inhibitory protein (cFLIP) and low levels of apoptosis (Caspase-8) and necroptosis (RIPK3) components. Cycloheximide treatment, which led to a reduction in cFLIP levels, rendered primary islets sensitive to TNF-induced cell death which was fully blocked by caspase inhibition.

Conclusions: Unlike in many other cell types (e.g., epithelial, and immune), RIPK1 is not required for cell death regulation in β-cells under physiological conditions or diabetic challenges. Moreover, *in vivo* and *in vitro* evidence suggest that pancreatic β-cells do not undergo necroptosis but mainly caspase-dependent death in response to TNF. Last, our results show that β-cells have a distinct mode of regulation of TNF-cytotoxicity that is independent of RIPK1 and that may be highly dependent on cFLIP.

Keywords RIPK1; Necroptosis; TNF; Apoptosis; β-cell; Diabetes; cFLIP

1. INTRODUCTION

Diabetes represents a group of metabolic disorders characterized by hyperglycemia due to defects in insulin production, sensing or both [1]. Type 1 diabetes is caused by autoimmune reaction towards insulin-producing β-cells [1] whereas type 2 diabetes is caused by insulin resistance which eventually leads to β-cell failure [2]. Although caused by different mechanisms, the key overlap between type 1 and type 2 diabetes is β-cell death. TNF is a proinflammatory cytokine which can induce inflammatory gene activation or cell death. The binding of TNF to TNFR1 induces the formation of complex-I which includes various prosurvival proteins, which act as checkpoints of TNF signalling, such as RIPK1 and the E3 ligases, cIAP1/2 and LUBAC [3]. This enables optimal gene activation by the NF-κB and MAPK pathways. Under certain conditions, for example, when any of these checkpoints are inhibited, RIPK1, via its kinase activity, autophosphorylates itself and

[1]Department of Translational Genomics, Faculty of Medicine, University of Cologne, Cologne, Germany [2]Centre for Molecular Medicine Cologne (CMMC), University of Cologne, Cologne, Germany [3]Cologne Excellence Cluster on Cellular Stress Responses in Aging-Associated Diseases (CECAD), Cologne, Germany [4]Inflammation and Cell Death Signalling group, Signal Transduction and Metabolism Laboratory, Université libre de Bruxelles, Brussels, Belgium [5]VIB Center for Inflammation Research, 9052 Ghent, Belgium [6]Department of Biomedical Molecular Biology, Ghent University, 9052 Ghent, Belgium [7]Institute for Genetics, University of Cologne, Cologne, Germany [8]Institute of Biochemistry I, Medical Faculty, University of Cologne, 50931 Cologne, Germany

*Corresponding author. Department of Translational Genomics, Faculty of Medicine, University of Cologne, Cologne, Germany. E-mails: m.peltzer@uni-koeln.de, n.peltzer@ibmg.uni-stuttgart.de (N. Peltzer).

Abbreviations: RIPK1, Receptor-interacting protein kinase 1; TNF, Tumor necrosis factor; TNFR1, Tumor necrosis factor receptor 1; cFLIP, Cellular FLICE (FADD-like IL-1β-converting enzyme)-inhibitory protein; RIPK3, Receptor-interacting protein kinase 3; LUBAC, Linear ubiquitin chain assembly complex; HOIP, HOIL-1 interacting protein; cIAP1/2, Cellular Inhibitor of Apoptosis Protein 1/2; MAPK, Mitogen-activated protein kinases; NF-κB, Nuclear factor 'kappa-light-chain-enhancer' of activated B-cells; TRAIL, TNF-related apoptosis ligand

Received February 2, 2024 • Revision received July 5, 2024 • Accepted July 6, 2024 • Available online 14 July 2024

https://doi.org/10.1016/j.molmet.2024.101988

induces the formation of complex-II. This complex can lead to apoptosis via Caspase-8. cFLIP (*CFLAR*) is a direct substrate and regulator of Caspase-8. It regulates levels of apoptosis by restraining the full activation of Caspase-8 [4]. Yet, the cFLIP/Caspase-8 heterodimer still bears sufficient activity to prevent another type of cell death called necroptosis [5]. When the activity of Caspase-8 is fully inhibited or absent, phosphorylated RIPK1 induces necroptosis via RIPK3 and MLKL [3,6]. In contrast to its kinase activity, the scaffolding function of RIPK1 is essential to limit cell death since loss of RIPK1 promotes both apoptosis and necroptosis leading to postnatal lethality in mice [7–9]. Hence, RIPK1 serves as a molecular switch regulating cell fate within TNF signalling and, as such, is tightly regulated [10].

TNF has been associated with β-cell loss and dysfunction [11,12]. Treatment with TNF-blocking monoclonal antibody in a cohort of 84 new-onset type 1 diabetes patients resulted in improved glucose metabolism [13]. Similarly, TNF blockade improved glucose metabolism and insulin resistance in rodent obesity models [14–16]. The mechanism of TNF-induced cell death is not fully characterised in β-cells despite the prominent role of TNF in diabetes pathogenesis [11,12]. In particular, the respective contribution of death receptor-induced apoptosis and necroptosis as well as the implication of RIPK1 function in type 1 diabetes are unclear. Gene variants of RIPK1 are associated with metabolic syndrome in humans, and RIPK1 depletion, but not the inhibition of its kinase activity, was shown to protect from metabolic syndrome in mice [17,18]. On the contrary, Necrostatin-1s, a RIPK1 kinase inhibitor, was shown to protect from metabolic syndrome [19]. To date, the role of RIPK1 scaffolding function in β-cells and diabetes remains unknown.

In the present study, we evaluated the role of RIPK1 in β-cell homeostasis by dissecting the contribution of its kinase versus scaffolding function under diabetic conditions. In line with previous reports, we show that the kinase activity of RIPK1 does not contribute to diabetes pathology. Crucially, our results demonstrate that β-cell survival is not affected by RIPK1 deficiency under basal conditions or upon diabetic challenges. Consequently, we conclude that β-cells are protected from the cytotoxic effect of TNF in the absence of RIPK1 possibly through high levels of anti-apoptotic cFLIP expression and poor expression of Caspase-8 and RIPK3.

2. RESEARCH DESIGN AND METHODS

2.1. Mice

Ripk1$^{\beta\text{-}KO}$ and *Hoip*$^{\beta\text{-}KO}$ mice were generated by crossing *Ripk1*$^{fl/fl}$ (Dannappel et al., 2014) and *Hoip*$^{fl/fl}$ [20], respectively, with B6(Cg)-Ins1tm1.1(cre)Thor/J (Thorens et al., 2015) mice kindly gifted by Hans Stauss (UCL, London, UK). *Ripk1*^{D138N} mice were previously described (Polykratis et al., 2014). FFPE samples from *Ripk3/Caspase-8* double knockout (DKO) and *Cflar;VillinCre-ERT2* mice were provided by Henning Walczak and Alessandro Annibaldi, respectively [21–23]. Mice were maintained in SPF animal facilities of CECAD research center. All experimental procedures were approved by local authorities (Landesamt für Natur, Umwelt und Verbraucherschutz Nordrhein-Westfalen) in Germany. The blood glucose levels and weight of *Ripk1*$^{\beta\text{-}KO}$ and *Hoip*$^{\beta\text{-}KO}$ mice were monitored weekly starting from 8 weeks of age. For this analysis, only female mice were utilized. The blood glucose was measured by using Adia Diabetes kit. For the Glucose Tolerance test (GTT), mice were orally administered with glucose at the dose of 2 g/kg (Sigma—Aldrich, G8769) after 6 h of fasting. For Insulin Tolerance Test (ITT), mice were injected intraperitoneally 0,75 U/kg after 6 h of fasting. For multiple low-dose Streptozotocin (MLDSTZ) model, male mice were injected either with citrate buffer, pH 4.5 or STZ with the dose of 50 mg/kg (Sigma—Aldrich, S0130) for 5 consecutive days. The mice were sacrificed at the experimental endpoint (20 days after the first injection) unless they reached the termination criteria (e.g. 20 % loss of the initial weight or blood glucose $>$ 600). For diet-induced obesity, the mice were fed with either a standard diet (10% kcal fat, Research Diets Inc, D12450B) or a high-fat diet (60% kcal fat, Research Diets Inc, D12492) for 20 weeks at the Inflammation Research Center from UGent-VIB (SPF animal facility) according to institutional, national and European animal regulations. A second cohort of 16-weeks of high fat diet feeding experiment was performed in CECAD ivRF. The mice were fed with either a standard diet (10% kcal fat, Research Diets Inc, D12450J) or a high-fat diet (60% kcal fat, Research Diets Inc, D12492). Only male mice were utilized for diet-induced obesity experiments.

2.2. Histological analysis, immunohistochemistry (IHC) and immunofluorescence (IF)

Following the tissue harvest, the pancreas was fixed overnight in a 10% neutral buffered formalin solution and paraffin embedded. For insulin (1:6400 diluted in Animal-Free Blocker, VEC-SP-5035, Vector Laboratories, C.S. C279) and CD45 (1:100, Thermofischer, 14-0451-82) IHC, antigen retrieval was done by using citrate buffer, pH 6 (Sigma—Aldrich, C9999) in pancreas sections (5 μM) by maintaining sub-boiling conditions in microwave for 5 min. For Caspase-8 (1:200, ALX-804-447-C100) and cFLIP (1:100, ab8421) IHC, antigen retrieval was done by using Tris—EDTA buffer, pH 9.5, in pancreas, spleen and colon sections by maintaining sub-boiling conditions in microwave for 10 min. The sections were incubated with BLOXALL Endogenous Blocking Solution (VEC-SP-6000, Vector Laboratories) to block endogenous peroxidases. This is followed by 30 min incubation with Animal-Free Blocker (VEC-SP-5035, Vector Laboratories). Following overnight incubation at 4 °C with primary antibodies, sections were washed with TBS-T (pH 7.6, 0.5 % Tween) 3 times for 10 min. Sections were incubated with immPRESS® HRP Goat Anti-Rabbit IgG Polymer Detection Kit, Peroxidase (MP-7451, Vector Laboratories) for 30 min. Following 3 times 10 min washes, the colour was developed by using HIGHDEF® DAB Chromogen/Substrate Set (ENZ-ACC105-0200, Enzo). The slides were scanned by slidescanner (Hamamatsu S360). The insulin + area was calculated by using QuPath0.4.0. For IF stainings, after antigen retrieval as described above, the sections were incubated with Animal-Free Blocker (VEC-SP-5035, Vector Laboratories) for 1 h at RT. For insulin-glucagon staining, primary antibodies insulin (1:100,5330-0104G, Bio-Rad) and glucagon (1:100, C.S. 2760) were incubated overnight at 4 °C, followed by washes as described above. The secondary antibodies (1:300, SA5-10094, Invitrogen and A-11011, Invitrogen) were used for insulin and glucagon respectively. After washes as described above, sections were counterstained with DAPI and mounted. For cl. Casp-3 staining, following the antigen retrieval as described above, sections were permeabilized with 0.2% triton in Animal-Free Blocker. The rest of the protocol was performed as described above using cl. Casp-3 antibody (1:50, C.S. 9661) and secondary antibody (1:300, A-11011, Invitrogen). The images were acquired by using STELLARIS 5 Confocal Microscope (Leica). The images were quantified by using FIJI and positive cells were counted manually. For cFLIP staining, antigen retrieval was done with Tris—EDTA buffer, pH 9.5. cFLIP antibody (1:100, ab8421) and the secondary antibody (1:300, A-1108, Invitrogen) was used as described above. The images were acquired by using STELLARIS 5 Confocal Microscope (Leica). The images were analyzed by QuPath0.4.0 using positive cell count command. Three different threshold values were set to detect different levels of fluorescence intensity.

2.3. Islet isolation, viability assay

For islet isolation, pancreas was digested in a water bath at 37 °C. Pancreatic islets were separated using density gradient (Histopaque-1077; Sigma Aldrich), followed by handpicking under microscope. Islets were cultured as described in [18]. The concentration of cytokines in the cocktail was used as follows: mTNF, 1000 U/mL (410-MT-025, R&D Systems), mIFN-γ, 1000 U/mL (315-05-100ug, Peprotech) and hIL-1β, 50 U/mL (201-LB-005, R&D Systems). TNF stimulation in primary islets was done using mTNF, 1000 U/mL (410-MT-025, R&D Systems). The final concentration of zVAD, Z-IETD-FMK and Smac mimetics were 50 μM, 50 μM and 5 μM, respectively (Selleck Chemicals). The final concentration of cycloheximide was 5 μg/mL (Merck, C7698-1G). The cell death in islets were determined by using propidium iodide (PI, 5 μg/mL, Sigma–Aldrich) and Hoechst 33342 (HO, 5 μg/mL, Sigma–Aldrich). Cell death levels in islets were assessed by two independent researchers and one of the researchers was not aware of the treatment conditions as performed in Takiishi et al. [18].

2.4. Western blot and ELISA

For western blot analysis, islets from *Ripk1*$^{\beta\text{-}KO}$ and control littermates were lysed in 30 mM Tris–Hcl, pH 7.5, 150 mM NaCl, 10 % glycerol, 1 % Triton X-100, 2 mM EDTA supplemented with PhosSTOP and cOmplete™, Mini Protease Inhibitor Cocktail (Roche). The denatured lysates were run using precast protein gels (4568084, Bio-rad) followed by transfer to the membrane (1704158, Bio-Rad). The membrane was incubated overnight at 4 °C with the primary RIPK1 antibody (BD, 610459), p-IκB (C.S. 9246), p-p65 (C.S. 3033), NF-κB p65 (C.S. 8242), total IκB (C.S. 9242), RIPK3 (ab62344), cFLIP (ab8421), cFLIP (C.S. 56343) Caspase-8 (MAB3429), insulin (BS-0862R). After the incubation with respective secondary antibody, color was developed using ECL (PerkinElmer, NEL103001EA). The serum insulin content of mice was quantified by insulin ELISA (Crystalchem, 90080). For qRT-PCR of the islets, RNA was extracted using Dynabeads™ mRNA DIRECT™ Purification Kit (61012). Reverse transcription was performed by using LunaScript RT SuperMix Kit (NEB #E3010) according to the manufacturer's protocol. For RT-PCR, Luna Universal qPCR Master Mix (NEB # M3003) was used. The primer sequences are as follow:

Target gene	Forward Primer (5′→3′)	Reverse Primer (5′→3′)
GAPDH	CTCCCACTCTTCCACCTTCG	GCCTCTCTTGCTCAGTGTCC
A20	CATGAAGCAAGAAGAACGGAAGA	GAGGCCCGGGCACATT
Fas	GCGGGTTCGTGAAACTGATAA	GCAAAATGGGCCTCCTTGATA
RIPK3	GAGATGGAAGACACGGCACT	GGTGGTGCTACCAAGGAGTT

2.5. scRNA-seq analysis of β-cells

For analysis of murine pancreatic islets expression, we utilized publicly available scRNA-seq data obtained from the National Center for Biotechnology Information (NCBI) Gene Expression Omnibus database under accession number GSE156175. Single-cell RNA sequencing of mouse islets exposed to proinflammatory cytokines [24]. Data Processing, quality control and normalization was performed as described in the original publication using R (R version 4.2.2) using the package Seurat (Version 4.2.0).

2.6. Tabula Muris analysis

The single-cell transcriptomic data used in this study was obtained from the FACS subset of Tabula Muris, a compendium of single-cell transcriptome data from male and female C57BL/6JN mice. The data was accessed from the Tabula Muris Consortium's public resource. The heatmaps were generated with the mean expression of each gene in specific cell types of each tissue. The Tabula Muris Consortium, Overall coordination, Logistical coordination. et al. Single-cell transcriptomics of 20 mouse organs creates a Tabula Muris. Nature 562, 367–372 (2018). https://doi.org/10.1038/s41586-018-0590-4.

2.7. Statistical analysis

Data was represented as Means ± SD and statistical analyses were carried out using GraphPad Prism 10.1.2. (GraphPad Software Inc., San Diego, CA, USA). Unpaired two-tailed t-test was carried out to compare the means of two groups. 2-way ANOVA was used to compare the means of groups with more than one variable. If a multiple comparison test was used, it is clarified in the figure legend. A $p < 0.05$ is considered statistically significant.

3. RESULTS

3.1. Lack of RIPK1-kinase activity does not affect onset and progression of MLDSTZ-induced diabetes

The kinase activity of RIPK1 was shown to be necessary for TNF-induced necroptosis and under certain conditions apoptosis [25]. To test whether RIPK1 kinase activity contributes to type 1 diabetes pathogenesis, we used RIPK1 kinase-inactive mice (*Ripk1*^{D138N}). *Ripk1*^{D138N} and WT mice were administered multiple low-dose streptozocin (MLDSTZ), and their blood glucose level was followed for 20 days (Figure 1A). *Ripk1*^{D138N} mice presented normal onset and progression of hyperglycemia upon MLDSTZ treatment (Figure 1A). At endpoint (20 days after the first injection or when the mice reached the termination criteria), we assessed islet composition by insulin-glucagon immunofluorescence (IF) staining and found that the β-cell (insulin-positive) or α-cell (glucagon-positive) ratio to total islet cells, and the total insulin-positive area were comparable between *Ripk1*^{D138N} and WT mice (Figure 1B and Fig. S1a). Since the kinase activity of RIPK1 can also promote apoptosis, we performed cleaved Caspase-3 (cl. Casp-3) staining. However, we observed similar levels of cl. Casp-3 positive cells in islets of *Ripk1*^{D138N} and WT mice (Figure 1C). We assessed insulitis upon MLDSTZ as described in Fig. S1b and did not observe any difference between the two genotypes (Figure 1D). These data indicate that RIPK1 kinase-dependent cell death does not contribute to type 1 diabetes onset and progression.

3.2. RIPK1 deficiency in β-cells does not cause spontaneous metabolic disorder

To study the role of RIPK1 scaffolding survival function in pancreatic β-cells, we generated *Ripk1*$^{\beta\text{-}KO}$ mice (specific deletion of RIPK1 in β-cells). The deletion of RIPK1 was confirmed by western blot from primary islets isolated from *Ripk1*$^{\beta\text{-}KO}$ and littermate controls (Figure 2A). *Ripk1*$^{\beta\text{-}KO}$ mice were normal weighed and presented normoglycemia throughout lifespan (Figure 2B,C). Moreover, neither young (8 weeks old) nor adult (30 weeks old) mutant animals showed glucose intolerance in glucose tolerance test (GTT) assays (Figure 2D,E). At 30 weeks of age, normal fed serum insulin levels in *Ripk1*$^{\beta\text{-}KO}$ mice were within normal range (Figure 2F). Moreover, *Ripk1*$^{\beta\text{-}KO}$ mice displayed normal islet structure (Figure 2G). To test whether β-cells have alternative mechanisms that protect them from loss of RIPK1, we deleted another key regulator of TNF signalling. HOIP is the main catalytic subunit of LUBAC, and its loss leads to cell death-dependent inflammation in cell types including endothelial cells and keratinocytes [20,26–28]. Deletion of HOIP in β-cells did not affect

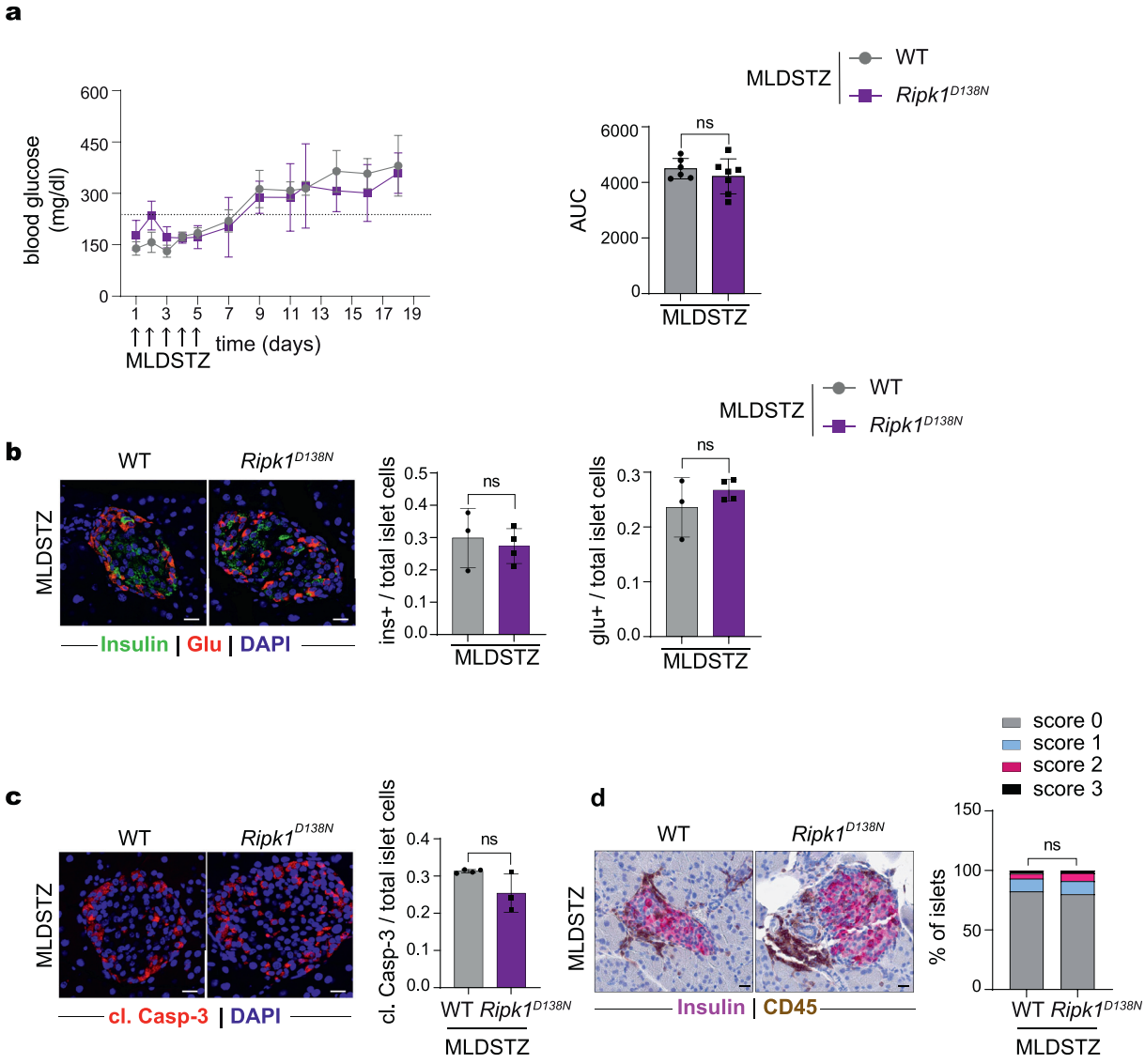

Figure 1: Kinase activity of RIPK1 does not affect type 1 diabetes onset and progression. *Ripk1*^{D138N} and WT controls were treated with MLDSTZ (50 mg/kg) for five consecutive days. **(A)** Fed-blood glucose levels were monitored over 20 days in (left) and area under the curve (AUC) was calculated (right) (n = 6–7). **(B)** Representative images of insulin and glucagon IF (left) and quantification of insulin and glucagon positive cells in islets of MLDSTZ-treated *Ripk1*^{D138N} and WT controls (n = 3–5 per group). **(C)** Representative images of cl. Casp-3 IF (left) and quantification of cl. Casp-3 positive cells in the islets of MLDSTZ-treated *Ripk1*^{D138N} and WT controls (n = 3–5 per group). **(D)** Representative images of insulin-CD45 staining and insulitis was graded as score 0, score 1, score 2, score 3. The representative images of MLDSTZ is selected from score 2 for each genotype. The percentage of each score was calculated for each group (n = 3–5 per group). Scale bars represents 20 μM. Means ± SD. Unpaired t-test (a, b, c). 2-way ANOVA with Tukey's multiple comparisons test (d).

normal-fed blood glucose levels, weight gain and glucose tolerance at different stages of life (Figs. S2a–d). Our results therefore suggest that RIPK1 and HOIP are dispensable for β-cell survival, development, and function in basal conditions.

3.3. Loss of RIPK1 in β-cells does not affect onset and progression of MLDSTZ-induced diabetes

To test whether RIPK1 scaffolding function is required to limit β-cell death during type 1 diabetes, we challenged the mice with MLDSTZ. The onset and progression of hyperglycemia was comparable between *Ripk1*$^{β\text{-}KO}$ and littermate controls (Figure 3A). Similarly, no difference was detected in blood glucose between *Hoip*$^{β\text{-}KO}$ mice and controls upon MLDSTZ (Fig. S2e). Fasting blood glucose levels, measured 10 days after the first STZ injection, were not affected by RIPK1 deficiency (Figure 3B). The mice were sacrificed 20 days after the first injection or when they reached the endpoint criteria according to animal welfare. The insulin-glucagon staining showed decreased β-cell ratio to total islet cells upon MLDSTZ regardless of the presence of RIPK1 (Figure 3C). Moreover, the insulin-positive area of MLDSTZ-treated *Ripk1*$^{β\text{-}KO}$ mice and littermate controls was similar (Fig. S3a). Since deficiency of RIPK1 induces apoptosis in certain cell types such as intestinal epithelial cells [29,30], we performed cl. Casp-3 staining to

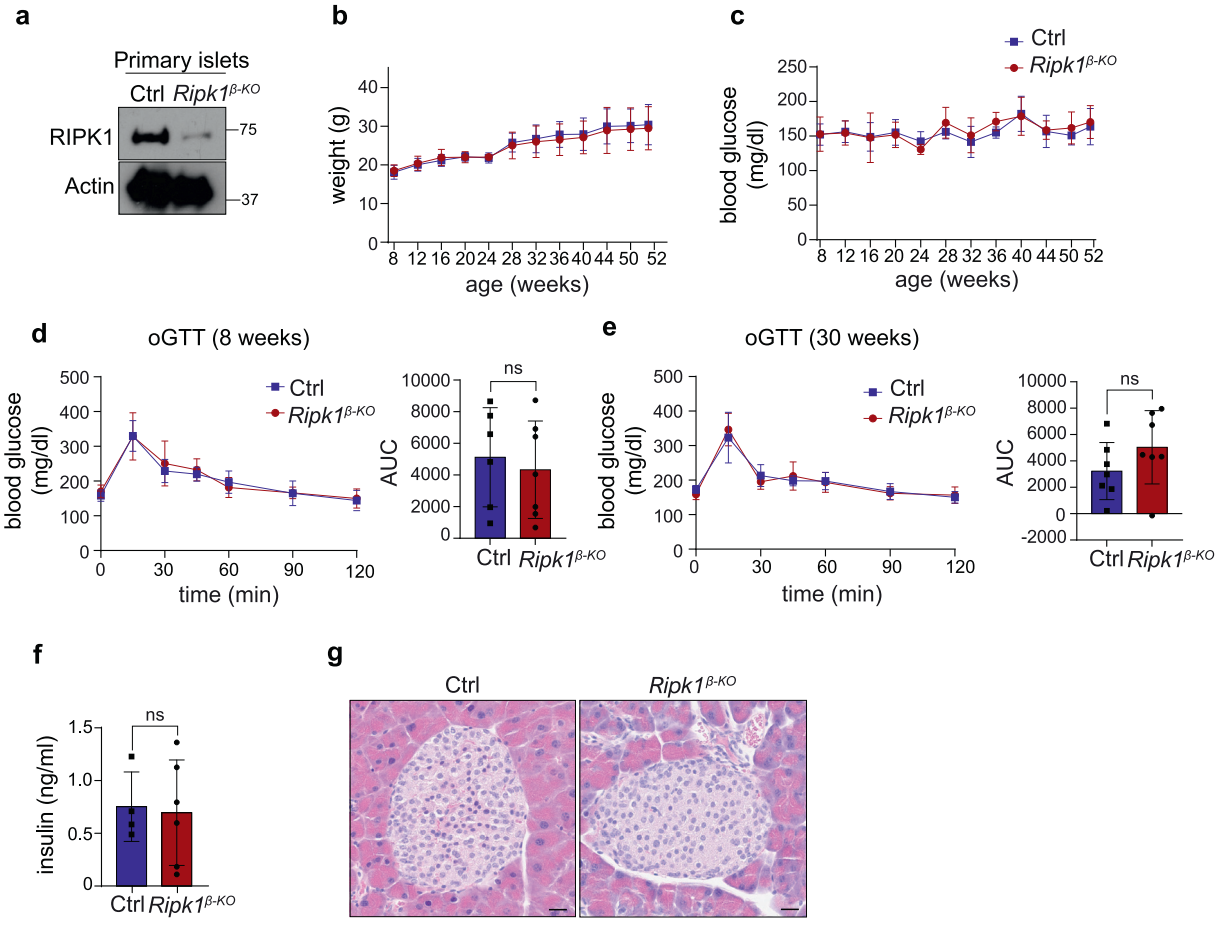

Figure 2: β-cell specific deletion of RIPK1 does not cause spontaneous metabolic disorder. (a) Deletion of RIPK1 is shown in primary islets from *Ripk1*$^{β\text{-}KO}$ and littermate controls by WB. **(b)** Body weight and **(c)** blood glucose were monitored weekly for 30 weeks in *Ripk1*$^{β\text{-}KO}$ and littermate controls (n = 15 per group). **(d,e)** Oral GTT (oGTT) in 8 weeks-old mice **(d)** and in 30-weeks old **(e)** *Ripk1*$^{β\text{-}KO}$ and littermate controls. Area under curve (AUC) is shown on the right of each histogram (n = 6–7 per group). **(f)** Fed serum insulin levels of 30-weeks old mice (n = 4–6). **(g)** Representative images of pancreatic islets stained with H&E. Scale bar represents 20 μM. Means ± SD. Unpaired t-test (d,e,f).

test whether loss of RIPK1 sensitised β-cells to apoptosis in response to MLDSTZ. Although we observed apoptosis induction upon MLDSTZ treatment, we failed to detect differences in cl. Casp-3 levels in *Ripk1*$^{β\text{-}KO}$ mice versus littermate controls (Figure 3D). *Ripk1*$^{β\text{-}KO}$ mice presented similar insulitis scores to their littermates (Figure 3E, S3b). Overall, our results indicate that RIPK1 scaffolding function, or HOIP, are not required for β-cell survival during MLDSTZ-induced diabetes.

3.4. Hyperglycemia induced by high-fat diet is not affected by RIPK1 deficiency

To understand the role of RIPK1 in a model of hyperglycemia, we used diet-induced obesity. *Ripk1*$^{β\text{-}KO}$ mice and littermate controls were fed a high-fat diet (HFD) for 20 weeks. No difference was observed in the weight gain between the two genotypes (Figure 4A). Glucose tolerance test performed at 10 weeks of HFD feeding showed that *Ripk1*$^{β\text{-}KO}$ mice were as glucose tolerant as their littermate controls (Figure 4B). In a different cohort of mice, *Ripk1*$^{β\text{-}KO}$ mice and littermate controls were fed with HFD for 16 weeks. In accordance with the previous cohort, we did not observe a difference between *Ripk1*$^{β\text{-}KO}$ mice and littermate controls in terms of weight gain, glucose and insulin tolerance at 16 weeks of HFD feeding (Figs. S4a–c). Our results suggest that deficiency of RIPK1 in β-cells does not affect diet-induced weight gain and hyperglycemia.

3.5. Resistance to TNF-induced cell death may be due to high cFLIP/Caspase-8 ratio and low RIPK3 expression

Next, we addressed whether β-cells lacking RIPK1 are sensitised to TNF-induced cell death *ex vivo*. We treated primary pancreatic islets with either TNF alone or in combination with Smac mimetics (S) to induce apoptosis by cIAP1/2 depletion or S + Zvad (Z) to induce necroptosis. Intriguingly, we found that pancreatic islets are resistant to TNF-induced apoptosis and necroptosis. Moreover, the deficiency of RIPK1 did not affect their sensitivity to TNF-induced apoptosis and necroptosis or to cytokine cocktail (TNF, IFNγ and IL-1β) (Figure 5A). The observation that pancreatic islets are not sensitive to TNF-induced cell death raised the question whether they respond to TNF at all. Stimulation of primary islets isolated from *Ripk1*$^{β\text{-}KO}$ mice and littermate controls with TNF, showed increased IκB and p65 phosphorylation and a mild increase in the expression of the NF-κB target genes, Fas and A20, suggesting that primary islets are responsive to TNF by activating NF-κB signaling pathway (Figs. S5a and b). It is important to note, that islets displayed a modest response to TNF, an observation that was previously reported [31]. Yet, there are no major differences in NF-κB activation in wildtype versus RIPK1-deficient islets. To better understand why RIPK1 does not act as a checkpoint in TNF-induced cell death, we analysed publicly available sc-RNA seq data of murine primary islets [24] (Figure 5B and S5c). We found that islet cells express very low to null levels of RIPK3 in

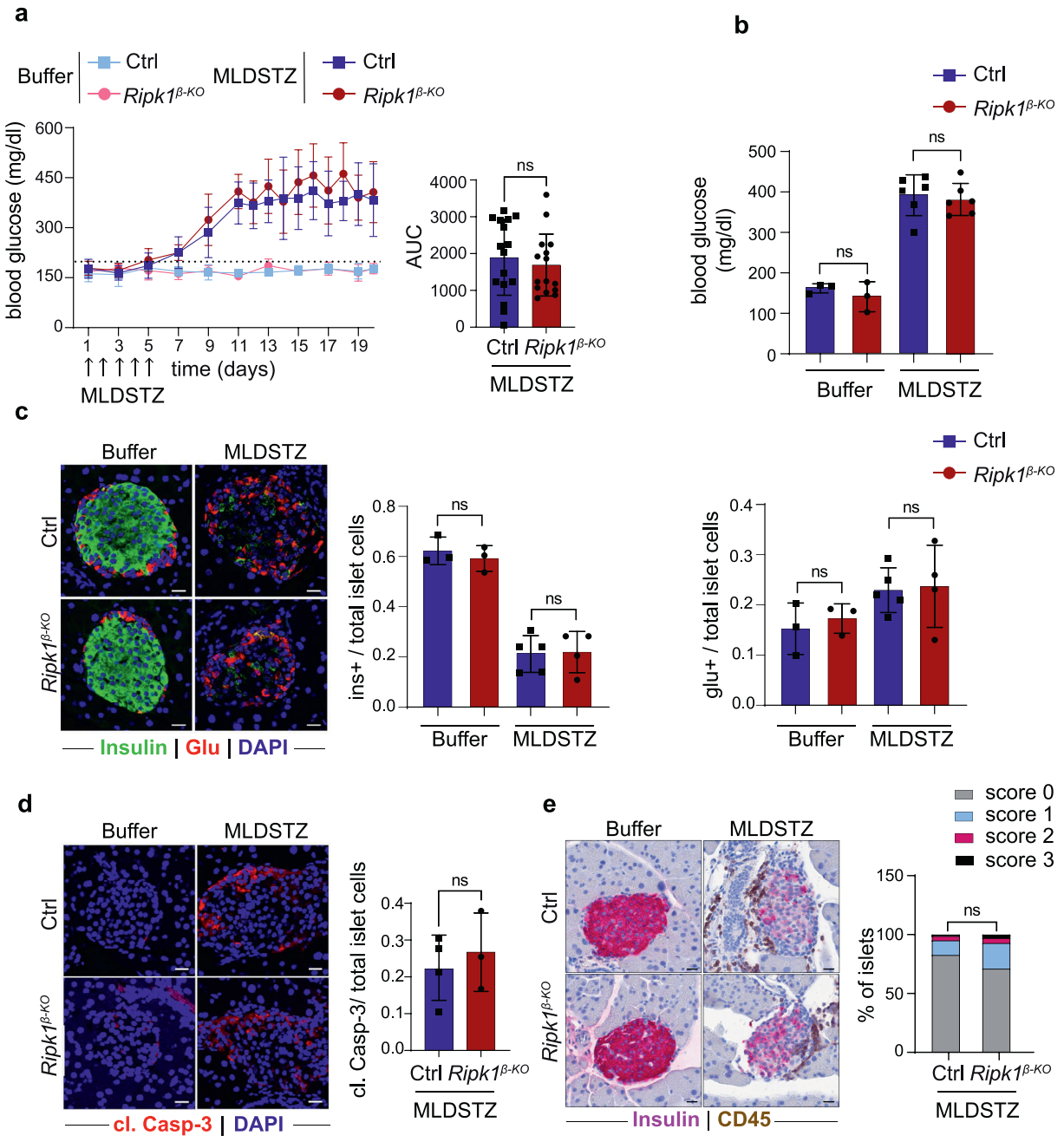

Figure 3: Type 1 diabetes onset and progression is not affected by loss of RIPK1 in β-cells. *Ripk1*$^{β\text{-}KO}$ and littermate controls were treated with citrate buffer or MLDSTZ. **(a)** Fed-blood glucose levels were monitored over 20 days in (left) and AUC was calculated (right) (n = 15–16 per group for MLDSTZ, n = 3 per group for buffer). **(b)** Fasting glucose levels at day 10 (n = 7 per group for MLDSTZ, n = 3 per group for buffer). **(c)** Representative images of insulin and glucagon IF (left) and quantification of insulin and glucagon positive cells in islets of buffer and MLDSTZ-treated *Ripk1*$^{β\text{-}KO}$ and littermate controls (n = 3–5 per group). **(d)** Representative images of cl. Casp-3 IF (left) and quantification of cl. Casp-3 positive cells in the islets of MLDSTZ-treated *Ripk1*$^{β\text{-}KO}$ and littermate controls. **(e)** Representative images of insulin-CD45 staining and insulitis was graded as score 0, score 1, score 2, score 3. The representative images of MLDSTZ is selected from score 2 for each genotype. The percentage of each score was calculated for each group (n = 3–5 per group). Scale bars represents 20 μM. Means ± SD. Unpaired t-test (a, b, c, d). 2-way ANOVA with Tukey's multiple comparisons test (e).

non-treated conditions or upon stimulation with IFNγ and/or IL1β which may explain why pancreatic islets do not undergo necroptosis (Figure 5B). Moreover, we found that β-cells express high levels of cFLIP and low levels of Caspase-8 under basal conditions (Figure 5B). Next, we compared cFLIP and Caspase-8 expression in various tissues that are known to be affected by TNF-induced cell death upon deficiency of RIPK1, such as colon, skin and bone marrow (Figure 5C, upper panel). Among these tissues, islet cells have distinctively high cFLIP expression as compared to Caspase-8 and hence a high CFLAR/Caspase-8 ratio (Figure 5C, lower panel). The same protein expression pattern was observed by cFLIP and Caspase-8 IHC stainings in pancreas, colon, and spleen (Figure 5D and Figs. S6a and b) and by western blot of isolated pancreatic islets (Figure 5E). This analysis revealed that islets express cFLIP under basal conditions but express very little, to undetectable,

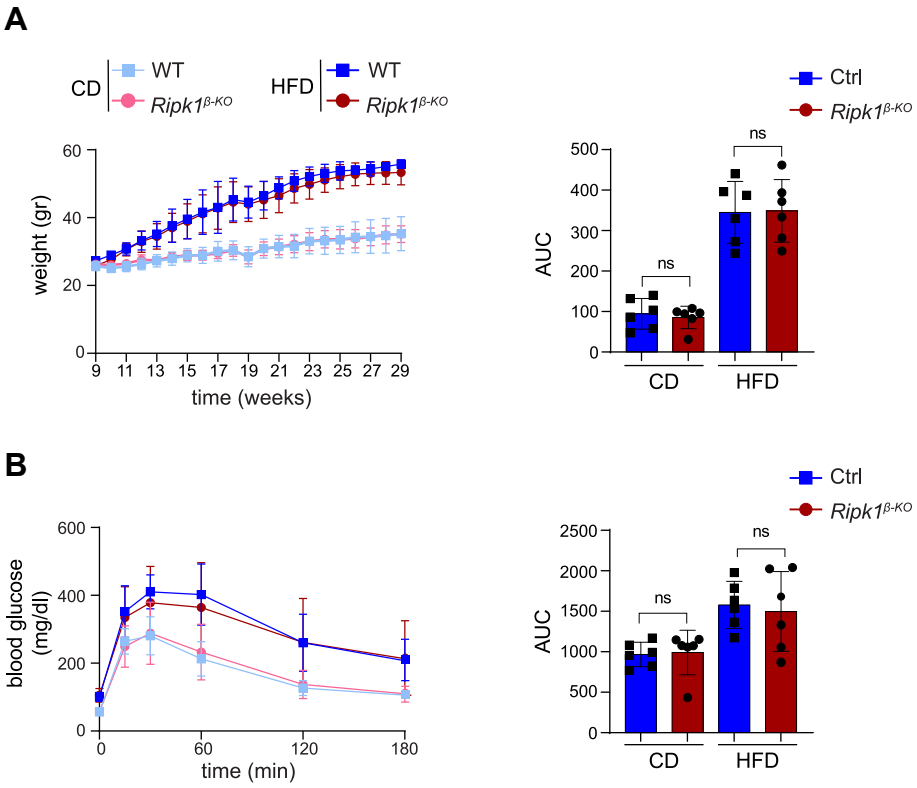

Figure 4: Hyperglycemia induced by HFD is not affected by RIPK1 deficiency in β-cells. *Ripk1*$^{\beta\text{-}KO}$ and littermate controls were fed with CD or HFD for 20 weeks. **(a)** Weekly body weight measurements (left) and AUC was calculated (right). **(b)** Intraperitoneal GTT (i.p.GTT) was performed at 10 weeks after the start of diet (left) and AUC was calculated (right) (n = 6 per group). Means ± SD. Unpaired t-test (a, b).

levels of Caspase-8 (Figure 5D). While MLDSTZ treatment in mice resulted in overexpression of cFLIP and Caspase-8 (Figs. S6a and b), TNF stimulation did not cause gross changes in their expression (Figure 5E), possibly explaining why there is cell death in MLDSTZ-treated islets as described above. No difference was observed in the expression levels of Caspase-8 and cFLIP between *Ripk1*$^{\beta\text{-}K0}$ mice and littermate controls (Fig. S6a,b,c). Low expression of RIPK3 was also observed in these datasets and confirmed by western blot and qRT-PCR of pancreatic islets as compared to mouse embryonic fibroblasts (Figs. S6d and e). Taken together, low to null RIPK3 expression and high cFLIP to Caspase-8 ratio can be a plausible explanation for resistance of islet cells to TNF-induced extrinsic cell death.

3.6. Cycloheximide treatment sensitises pancreatic islets to TNF-induced cell death

Since we hypothesise that high cFLIP/Caspase-8 ratio protects β-cells to TNF-induced cell death, we tested whether cFLIP depletion by cycloheximide (CHX) treatment would, differently from smac mimetics (SM), render β-cells sensitive to TNF-induced cell death. CHX treatment efficiently reduced cFLIP protein levels after 24 hs (Figure 6A). In line with cFLIP depletion, TNF plus CHX treatment, but not CHX alone, induced cell death in pancreatic islets (Figure 6B,C) and as previously reported [32]. Notably, cell death was induced by TNF + CHX treatment but not by TNF + S (Figures 5A and 6B,C and S7). Moreover, TNF + CHX-induced cell death was completely prevented by the pan-caspase inhibitor zVAD or the Caspase-8 inhibitor, zIETD-FMK. This indicates that β-cells die mainly by apoptosis in response to TNF and that necroptosis does not occur even when cells are licensed to die. Of note, under conditions that efficiently induce cell death in pancreatic islets, we could not observe differences between wildtype and *Ripk1*$^{\beta\text{-}K0}$ islets, providing further evidence that TNF-induced cell death is independent of RIPK1 in these cells.

4. DISCUSSION

TNF has long been associated with β-cell death, however, the mechanisms involved are not well-characterised. Moreover, the contribution of different cell death modalities to diabetes pathogenesis is not known. β-cell-specific deletion of Caspase-8 protected mice from MLDSTZ-induced diabetes indicates that extrinsic apoptosis contributes to the disease. However, these mice develop spontaneous hyperglycemia with ageing, accompanied by increased cell death in the islets which could be explained by necroptosis induction in the absence of Caspase-8 [33]. Although constitutive RIPK3 deficiency was shown to protect mice from MLDSTZ-induced diabetes [34], in a transplantation model, pancreatic islets lacking RIPK3 were as sensitive to T-cell killing as wild type islets, excluding a role of necroptosis in autoimmune diabetes [35]. Our study is in line with the latter and with Takiishi et al. who showed that RIPK1-mediated cell death does not play a role in type 1 diabetes by using *Ripk1*^{S25D} mice under the same type 1 diabetes challenge [18]. In addition, Karunakaran et al. reported that RIPK1 kinase inactive mice, *Ripk1*^{K45A}, are not protected from diet-induced metabolic syndrome [17]. We also demonstrated *ex vivo* that TNF-induced cell death induced by sensitisation with CHX, was fully blocked, rather than exacerbated, by caspase inhibition, providing further evidence that necroptosis does not occur in β-cells.

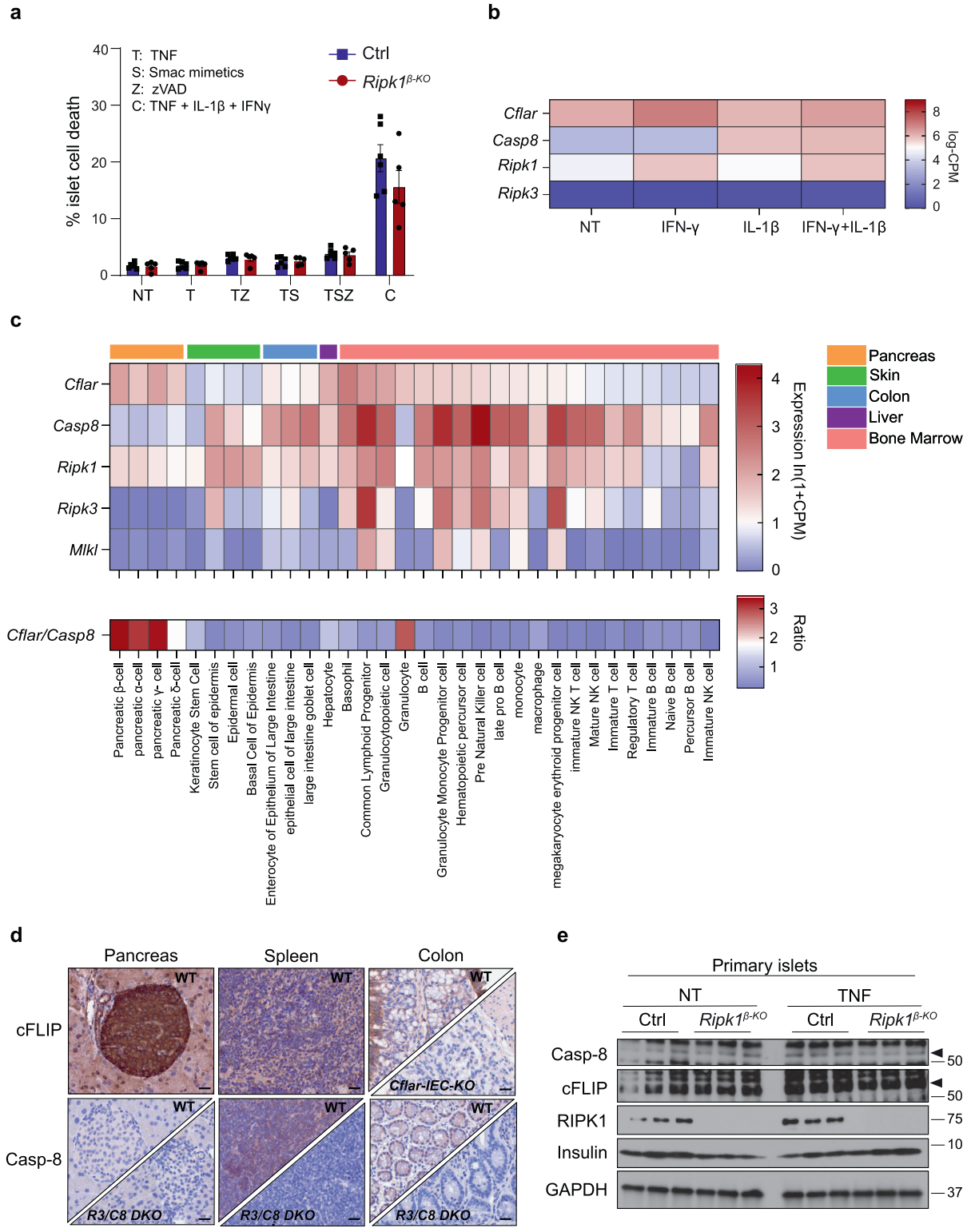

Figure 5: Pancreatic islets are not sensitive to TNF-induced cell death; potentially explained by lack of RIPK3 and high cFLIP expression.
(a) Percentage of cell death in mouse primary islets isolated from *Ripk1*$^{\beta\text{-KO}}$ and littermate controls treated with TNF (T), TNF and zVAD (TZ), TNF and Smac mimetics (TS), TNF, Smac mimetics and zVAD (TSZ), Cocktail with IL-1β, TNF, IFNγ (C) for 24 h (n = 5–6 per group). **(b)** Gene expression profile of indicated genes from mouse β-cells treated with IL-1β, IFNγ, IL-1β + IFNγ for 6 h or non-treated (NT). **(c)** Expression levels of indicated genes across different organs and cell types from the *Tabula Muris* dataset (upper panel). Ratio of cFLIP (*Cflar*) to Caspase-8 (*Casp8*) expression level in indicated organs and cell types **(d)** IHC staining of Caspase-8 and cFLIP in pancreas, colon and spleen. *R3/C8 DKO* stands for *Casp8/Ripk3* constitutive knockout (upper panel) and *Cflar-IEC-KO* (Cflar deletion in intestinal epithelial cells) (bottom right). Scale bars represent 20 μm. Chromogen (DAB) incubation was done equally in different tissues. **(e)** Primary islets isolated from *Ripk1*$^{\beta\text{-KO}}$ mice and littermate controls (n = 3 per genotype) were stimulated with TNF for 24 h. The expression levels of indicated proteins were analysed by western blotting.

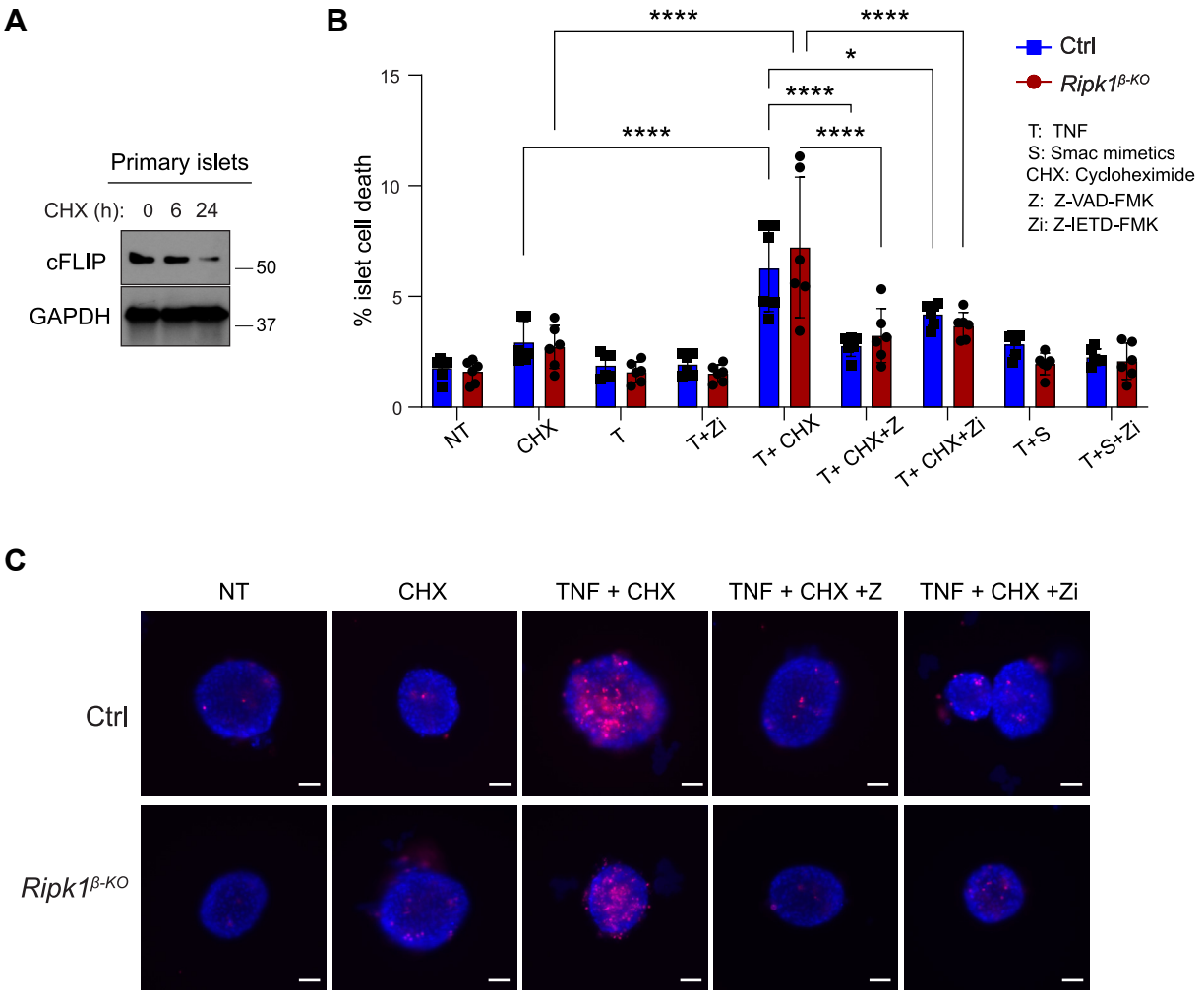

Figure 6: Cycloheximide treatment renders pancreatic islets sensitive to TNF-induced cell death, an implication of c-FLIP. (a) Primary islets were treated with CHX for 6 h or 24 h and cFLIP levels were analysed by western blotting. (b) Percentage of cell death in mouse primary islets isolated from *Ripk1*$^{\beta\text{-}KO}$ and littermate controls treated with the indicated conditions for 24 h (n = 6 per group). (c) Representative images of islets after 24 h of treatment with the indicated conditions. Scale bars represent 100 μm. Means ± SD. 2-way ANOVA with Šídák's multiple comparisons test. *p < 0.05, **p < 0.01, ***p < 0.001, ****p < 0.0001.

Furthermore, Takiishi et al. showed that necroptotic stimuli do not translate into cell death although RIPK1 is phosphorylated, suggesting that β-cells have a mechanism downstream RIPK1 activation that protects from TNF-induced cell death.

Intriguingly, unlike many other cell types, we found that β-cells are not sensitive to cell death upon deletion of RIPK1 or HOIP under physiological conditions and diabetic challenges. It is particularly intriguing in the context of type 1 diabetes because Caspase-8 deficiency in β-cells protects from MLDSTZ-induced diabetes [33], indicating that death receptor-associated cell death machinery is engaged in this model. Curiously, it has been shown that death ligands such as TRAIL and FasL are dispensable for T-cell killing of β-cells [36,37]. Similarly, we and others showed that intact pancreatic islets are not sensitive to TNF along with cIAP1/2 depletion which is a widely used extrinsic apoptosis stimulus [18]. To understand what could be the mechanism that sustains β-cells survival upon check-point inhibition within the TNF pathway such as LUBAC deficiency, cIAP1/2 depletion and RIPK1 phosphorylation, we examined the expression profile of cell death proteins in β-cells. We found that β-cells express extremely low levels of MLKL and RIPK3. This goes in line with the observed negligible role of RIPK1 kinase activity in diabetes onset as discussed above. Moreover, we showed that β-cells express distinctively high levels of cFLIP compared to Caspase-8. The latter could represent a mechanism by which β-cells prevent TNF-induced cytotoxicity in conditions that were reported to licence TNF to kill in many other cell types and organs. Indeed, we found that CHX treatment which correlated with a depletion in cFLIP, sensitised cells to TNF-induced cell death. This goes in line with a report showing that overexpression of cFLIP in β-cell lines protects from TNF- and cytokine-induced cell death [38]. Although our data places cFLIP as the main checkpoint in TNF-cytotoxicity in β-cells, we cannot exclude the possibility that CHX also targets other prosurvival factors that are important to preserve β-cell survival, e.g. MCL1 [39,40]. Hence, the prominent role of cFLIP in β-cell death regulation, homeostasis and during pathological conditions warrants further investigation.

On one hand, high levels of cFLIP could explain why β-cells are protected from TNF-induced cell death. On the other hand, evidence suggests that Caspase-8 deletion in β-cells protects from diabetes onset [33]. Hence, how Caspase-8 gets activated in the presence of overwhelmingly high levels of cFLIP, especially upon MLDSTZ challenge, remains an open question. It is important to note that Caspase-8

expression was also increased upon MLDSTZ treatment, hence becoming available for activation. Emerging evidence suggests that Caspase-8 can be cleaved in an iNOS-dependent manner [41,42]. Considering the prominent role of iNOS in β-cell demise [43–45], and the fact that *Nos2* expression is induced by cytokine cocktail (Fig. S6a), it is possible that Caspase-8 cleavage and activation during diabetes occurs in an iNOS and NO-dependent manner potentially bypassing the inhibitory effect of cFLIP over Caspase-8. Overall, our results indicate that β-cells are resistant to TNF-induced apoptosis and necroptosis, upon loss of key survival nodes in TNF signalling, which can be a pro-survival adaptation in order to protect β-cell mass and maintain normoglycemia upon a plethora of inflammatory conditions.

CREDIT AUTHORSHIP CONTRIBUTION STATEMENT

Önay Veli: Writing – review & editing, Writing – original draft, Methodology, Investigation, Funding acquisition, Conceptualization. **Öykü Kaya:** Methodology. **Ana B. Varanda:** Software, Methodology. **Ximena Hildebrandt:** Methodology. **Peng Xiao:** Methodology. **Yann Estornes:** Methodology. **Matea Poggenberg:** Resources, Methodology. **Yuan Wang:** Methodology. **Manolis Pasparakis:** Resources. **Mathieu J.M. Bertrand:** Methodology. **Henning Walczak:** Resources. **Alessandro Annibaldi:** Writing – review & editing, Resources, Methodology. **Alessandra K. Cardozo:** Writing – review & editing, Methodology. **Nieves Peltzer:** Writing – review & editing, Writing – original draft, Supervision, Methodology, Funding acquisition, Conceptualization.

ACKNOWLEDGEMENTS

We would like to thank all members of the Annibaldi, Liccardi and Walczak labs for sharing reagents and for helpful discussions. We particularly thank Erick Arroba and Anne Van Praet from A.K.C. group for their help with experiments with primary islets. We thank Hans Stauss for gifting Ins1-Cre mice and Lucy Walker and Chunjing Wang for protocols and discussions. We also thank the CECAD ivRF, CECAD Imaging facility and SFB1403 Histology Facility for their support. We thank Emma Deblangy for proofreading the manuscript. This work is supported by the Deutsche Forschungsgemeinschaft (DFG) (SFB1403 [414786233] to NP, HW and MP, SFB1399 [413326622] to NP, HW and MP, SFB1530 [455784452] to NP, HW and AA) and the NRW Network consortium CANTAR (NW21-062B) to NP, HW and AA. NP is further supported by the Center for Molecular Medicine Cologne, Career Advancement Program and by the Jurgen Manchot Stiftung (JMSF). Ö.V. is supported by JMSF [4002-9502-0001]. Work in the A.K.C. group was supported by Fonds National de la Recherche Scientifique (FNRS CDR J.0109.220). H.W. is supported by the Wellcome Trust Investigator Award (214342/Z/18/Z). Research in the M.J.M.B. group is supported by grants from FWO-Vlaanderen (3G046420, 3G044518W, EOS CD-INFLADIS (3G0I5722)) and Ghent University (iBOF ATLANTIS grant 01IB3920, 01G00123).

DECLARATION OF COMPETING INTEREST

The authors declare that they have no known competing financial interests or personal relationships that could have appeared to influence the work reported in this paper.

DATA AVAILABILITY

Data will be made available on request.

APPENDIX A. SUPPLEMENTARY DATA

Supplementary data to this article can be found online at https://doi.org/10.1016/j.molmet.2024.101988.

REFERENCES

[1] Katsarou A, Gudbjörnsdottir S, Rawshani A, Dabelea D, Bonifacio E, Anderson BJ, et al. Type 1 diabetes mellitus. Nat Rev Dis Prim 2017;3:17016.
[2] DeFronzo RA, Ferrannini E, Groop L, Henry RR, Herman WH, Holst JJ, et al. Type 2 diabetes mellitus. Nat Rev Dis Prim 2015;1:15019.
[3] Peltzer N, Walczak H. Cell death and inflammation–a vital but dangerous liaison. Trends Immunol 2019;40(5):387–402.
[4] Martinez Lagunas K, Savcigil DP, Zrilic M, Carvajal Fraile C, Craxton A, Self E, et al. Cleavage of cFLIP restrains cell death during viral infection and tissue injury and favors tissue repair. Sci Adv 2023;9(30):eadg2829.
[5] Oberst A, Dillon CP, Weinlich R, McCormick LL, Fitzgerald P, Pop C, et al. Catalytic activity of the caspase-8–FLIPL complex inhibits RIPK3-dependent necrosis. Nature 2011;471(7338):363–7.
[6] Delanghe T, Dondelinger Y, Bertrand MJM. RIPK1 kinase-dependent death: a symphony of phosphorylation events. Trends Cell Biol 2020;30(3):189–200.
[7] Dillon CP, Weinlich R, Rodriguez DA, Cripps JG, Quarato G, Gurung P, et al. RIPK1 blocks early postnatal lethality mediated by caspase-8 and RIPK3. Cell 2014;157(5):1189–202.
[8] Kelliher MA, Grimm S, Ishida Y, Kuo F, Stanger BZ, Leder P. The death domain kinase RIP mediates the TNF-induced NF-kappaB signal. Immunity 1998;8(3):297–303.
[9] Rickard JA, O'Donnell JA, Evans JM, Lalaoui N, Poh AR, Rogers T, et al. RIPK1 regulates RIPK3-MLKL-driven systemic inflammation and emergency hematopoiesis. Cell 2014;157(5):1175–88.
[10] Huyghe J, Priem D, Bertrand MJM. Cell death checkpoints in the TNF pathway. Trends Immunol 2023. https://doi.org/10.1016/j.it.2023.05.007.
[11] Kim H-E, Choi S-E, Lee S-J, Lee J-H, Lee Y-J, Kang SS, et al. Tumour necrosis factor-α-induced glucose-stimulated insulin secretion inhibition in INS-1 cells is ascribed to a reduction of the glucose-stimulated Ca2+ influx. J Endocrinol 2008;198(3):549–60.
[12] Tai N, Wong FS, Wen L. The role of the innate immune system in destruction of pancreatic beta cells in NOD mice and humans with type I diabetes. J Autoimmun 2016;71:26–34.
[13] Quattrin T, Haller MJ, Steck AK, Felner EI, Li Y, Xia Y, et al. Golimumab and beta-cell function in youth with new-onset type 1 diabetes. N Engl J Med 2020;383(21):2007–17.
[14] Liang H, Yin B, Zhang H, Zhang S, Zeng Q, Wang J, et al. Blockade of tumor necrosis factor (TNF) receptor type 1-mediated TNF-alpha signaling protected Wistar rats from diet-induced obesity and insulin resistance. Endocrinology 2008;149(6):2943–51.
[15] Borst SE, Bagby GJ. Neutralization of tumor necrosis factor reverses age-induced impairment of insulin responsiveness in skeletal muscle of Sprague-Dawley rats. Metab Clin Exp 2002;51(8):1061–4.
[16] Uysal KT, Wiesbrock SM, Marino MW, Hotamisligil GS. Protection from obesity-induced insulin resistance in mice lacking TNF-alpha function. Nature 1997;389(6651):610–4.
[17] Karunakaran D, Turner AW, Duchez A-C, Soubeyrand S, Rasheed A, Smyth D, et al. RIPK1 gene variants associate with obesity in humans and can be therapeutically silenced to reduce obesity in mice. Nat Metab 2020;2(10):1113–25.
[18] Takiishi T, Xiao P, Franchimont M, Gilglioni EH, Arroba EN, Gurzov EN, et al. Inhibition of RIPK1 kinase does not affect diabetes development: β-Cells survive RIPK1 activation. Mol Metabol 2023;69:101681.

[19] Xu H, Du X, Liu G, Huang S, Du W, Zou S, et al. The pseudokinase MLKL regulates hepatic insulin sensitivity independently of inflammation. Mol Metabol 2019;23:14—23.
[20] Peltzer N, Rieser E, Taraborrelli L, Draber P, Darding M, Pernaute B, et al. HOIP deficiency causes embryonic lethality by aberrant TNFR1-mediated endothelial cell death. Cell Rep 2014;9(1):153—65.
[21] Newton K, Sun X, Dixit VM. Kinase RIP3 is dispensable for normal NF-κBs, signaling by the B-cell and T-cell receptors, tumor necrosis factor receptor 1, and toll-like receptors 2 and 4. Mol Cell Biol 2004;24(4):1464—9.
[22] Salmena L, Lemmers B, Hakem A, Matysiak-Zablocki E, Murakami K, Au PYB, et al. Essential role for caspase 8 in T-cell homeostasis and T-cell-mediated immunity. Gene Dev 2003;17(7):883—95.
[23] el Marjou F, Janssen K-P, Chang BH-J, Li M, Hindie V, Chan L, et al. Tissue-specific and inducible Cre-mediated recombination in the gut epithelium. Genesis 2004;39(3):186—93.
[24] Stancill JS, Kasmani MY, Khatun A, Cui W, Corbett JA. Single-cell RNA sequencing of mouse islets exposed to proinflammatory cytokines. Life Sci Alliance 2021;4(6). https://doi.org/10.26508/lsa.202000949.
[25] Polykratis A, Hermance N, Zelic M, Roderick J, Kim C, Van T-M, et al. Cutting edge: RIPK1 Kinase inactive mice are viable and protected from TNF-induced necroptosis in vivo. J Immunol 2014;193(4):1539—43.
[26] Taraborrelli L, Peltzer N, Montinaro A, Kupka S, Rieser E, Hartwig T, et al. LUBAC prevents lethal dermatitis by inhibiting cell death induced by TNF, TRAIL and CD95L. Nat Commun 2018;9(1):3910.
[27] Shimizu Y, Peltzer N, Sevko A, Lafont E, Sarr A, Draberova H, et al. The Linear ubiquitin chain assembly complex acts as a liver tumor suppressor and inhibits hepatocyte apoptosis and hepatitis. Hepatology 2017;65(6):1963—78.
[28] Sakamoto Y, Sasaki K, Omatsu M, Hamada K, Nakanishi Y, Itatani Y, et al. Differential involvement of LUBAC-mediated linear ubiquitination in intestinal epithelial cells and macrophages during intestinal inflammation. J Pathol 2023;259(3):304—17.
[29] Dannappel M, Vlantis K, Kumari S, Polykratis A, Kim C, Wachsmuth L, et al. RIPK1 maintains epithelial homeostasis by inhibiting apoptosis and necroptosis. Nature 2014;513(7516):90—4.
[30] Takahashi N, Vereecke L, Bertrand MJM, Duprez L, Berger SB, Divert T, et al. RIPK1 ensures intestinal homeostasis by protecting the epithelium against apoptosis. Nature 2014;513(7516):95—9.
[31] Ortis F, Cardozo AK, Crispim D, Störling J, Mandrup-Poulsen T, Eizirik DL. Cytokine-induced proapoptotic gene expression in insulin-producing cells is related to rapid, sustained, and nonoscillatory nuclear factor-kappaB activation. Mol Endocrinol 2006;20(8):1867—79.
[32] McKenzie MD, Carrington EM, Kaufmann T, Strasser A, Huang DCS, Kay TWH, et al. Proapoptotic BH3-only protein Bid is essential for death receptor-induced apoptosis of pancreatic beta-cells. Diabetes 2008;57(5):1284—92.
[33] Liadis N, Salmena L, Kwan E, Tajmir P, Schroer SA, Radziszewska A, et al. Distinct in vivo roles of caspase-8 in beta-cells in physiological and diabetes models. Diabetes 2007;56(9):2302—11.
[34] Contreras CJ, Mukherjee N, Branco RCS, Lin L, Hogan MF, Cai EP, et al. RIPK1 and RIPK3 regulate TNFα-induced β-cell death in concert with caspase activity. Mol Metabol 2022;65:101582.
[35] Zhao Y, Scott NA, Fynch S, Elkerbout L, Wong WW-L, Mason KD, et al. Autoreactive T cells induce necrosis and not BCL-2-regulated or death receptor-mediated apoptosis or RIPK3-dependent necroptosis of transplanted islets in a mouse model of type 1 diabetes. Diabetologia 2015;58(1):140—8.
[36] Knight RR, Kronenberg D, Zhao M, Huang GC, Eichmann M, Bulek A, et al. Human β-cell killing by autoreactive preproinsulin-specific CD8 T cells is predominantly granule-mediated with the potency dependent upon T-cell receptor avidity. Diabetes 2013;62(1):205—13.
[37] Apostolou I, Hao Z, Rajewsky K, von Boehmer H. Effective destruction of Fas-deficient insulin-producing beta cells in type 1 diabetes. J Exp Med 2003;198(7):1103—6.
[38] Cottet S, Dupraz P, Hamburger F, Dolci W, Jaquet M, Thorens B. cFLIP protein prevents tumor necrosis factor-alpha-mediated induction of caspase-8-dependent apoptosis in insulin-secreting betaTc-Tet cells. Diabetes 2002;51(6):1805—14.
[39] Stewart DP, Koss B, Bathina M, Perciavalle RM, Bisanz K, Opferman JT. Ubiquitin-independent degradation of antiapoptotic MCL-1. Mol Cell Biol 2010;30(12):3099—110.
[40] Meyerovich K, Violato NM, Fukaya M, Dirix V, Pachera N, Marselli L, et al. MCL-1 is a key antiapoptotic protein in human and rodent pancreatic β-cells. Diabetes 2017;66(9):2446—58.
[41] Simpson DS, Pang J, Weir A, Kong IY, Fritsch M, Rashidi M, et al. Interferon-γ primes macrophages for pathogen ligand-induced killing via a caspase-8 and mitochondrial cell death pathway. Immunity 2022;55(3):423—441.e9.
[42] Dubey M, Nagarkoti S, Awasthi D, Singh AK, Chandra T, Kumaravelu J, et al. Nitric oxide-mediated apoptosis of neutrophils through caspase-8 and caspase-3-dependent mechanism. Cell Death Dis 2016;7(9):e2348.
[43] Oyadomari S, Takeda K, Takiguchi M, Gotoh T, Matsumoto M, Wada I, et al. Nitric oxide-induced apoptosis in pancreatic β cells is mediated by the endoplasmic reticulum stress pathway. Proc Natl Acad Sci USA 2001;98(19):10845—50.
[44] Liu D, Pavlovic D, Chen MC, Flodström M, Sandler S, Eizirik DL. Cytokines induce apoptosis in beta-cells isolated from mice lacking the inducible isoform of nitric oxide synthase (iNOS-/-). Diabetes 2000;49(7):1116—22.
[45] Meyerovich K, Ortis F, Allagnat F, Cardozo AK. Endoplasmic reticulum stress and the unfolded protein response in pancreatic islet inflammation. J Mol Endocrinol 2016;57(1):R1—17.

